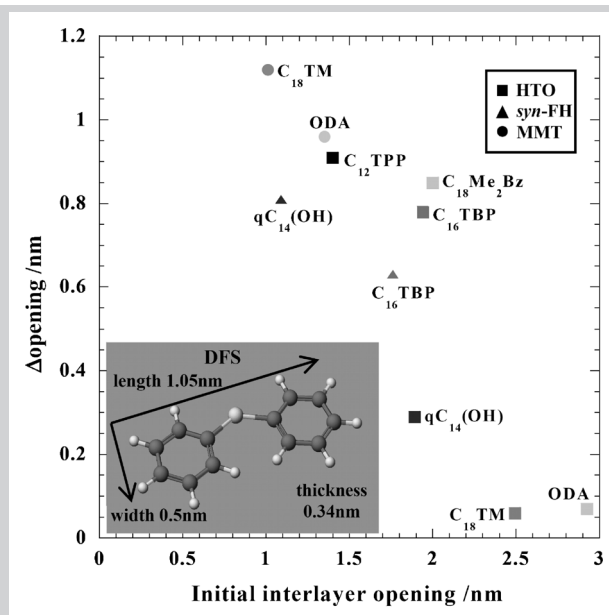


Summary: For the reference system of PPS-based nanocomposites, we investigated the intercalation behavior of DFS molecules into nano galleries based on OMLFs consisting of different types of intercalants and nanofillers with different surface charge densities. The smaller initial interlayer opening led to the larger interlayer expansion, regardless of the miscibility between the intercalant and DFS. We examined the preparation of PPS-based nanocomposites with and/or without shear processing at 300 °C. The finer dispersion of OMLFs in the nanocomposite was observed when using OMLF having small initial interlayer opening. The delamination of the stacked nanofillers was governed by the initial interlayer opening, whereas the uniform dispersion of the nanofillers was affected by the shear.



Plot of initial interlayer opening versus Δ opening for various OMLFs intercalated with DFS.

Intercalation of Diphenyl Sulfide into Nanogalleries and Preparation of Poly(*p*-phenylenesulfide)-Based Nanocomposites

Tomotaka Saito,¹ Masami Okamoto,*¹ Ryoichi Hiroi,² Minoru Yamamoto,² Takashi Shiroy²

¹Advanced Polymeric Nanostructured Materials Engineering, Graduate School of Engineering, Toyota Technological Institute, Hisakata 2-12-1, Tempaku, Nagoya 468-8511, Japan

Fax: +81 052 809 1864; E-mail: okamoto@toyota-ti.ac.jp

²Advanced Material Products Group, Research & Technical Center, Otsuka Chemicals Co. Ltd., Kagasuno Kawauchi-Cho 463, Tokushima 771-0193, Japan

Received: July 19, 2006; Revised: September 1, 2006; Accepted: September 1, 2006; DOI: 10.1002/mame.200600287

Keywords: interdigitated layer structure; melt; nanocomposites; poly(*p*-phenylenesulfide); surface charge density

Introduction

Continued progress in nanoscale controlling, as well as an improved understanding of the physicochemical phenomena at the nano galleries of the layered silicates, have contributed to the rapid development of polymer/layered silicate nanocomposites.^[1]

In order to understand the thermodynamic issue associated with nanocomposites formation, Vaia et al. applied

the mean-field statistical lattice model, and they found conclusions based on the mean-field theory to agree with the experimental results.^[2,3] In the study, the entropy loss associated with the confinement of a polymer melt is not prohibited to nanocomposite formation because an entropy gain associated with the layer separation balances the entropy loss of polymer intercalation, resulting in a net entropy change near to zero. Thus, from the theoretical model, the outcome of nanocomposite formation via

polymer melt intercalation depends on energetic factors, which may be determined from the surface energies of the polymer and organically modified layered filler (OMLF).

Nevertheless, we have often faced the problem that the nanocomposite shows a fine and homogeneous distribution of the nano particles in the polymer matrix [e.g., poly(L-lactide)] without a clear peak shift of the mean interlayer spacing of the (001) plane, as revealed by wide-angle X-ray diffraction (WAXD) analysis.^[4] Furthermore, we sometimes encounter a decrease in the interlayer spacing compared with that of pristine OMLF, despite very fine dispersion of the silicate particles. To the best of our knowledge, the mechanism of the direct melt intercalation in the nanocomposite formation is very complicated, and is not very well explored in the literature.

In this regard, we reported previously that an optimal interlayer structure on OMLF is most favorable for nanocomposite formation with respect to the number per area and size of the surfactant (intercalant) chains^[5,6]. In the study, we supported the interdigitated layer structure model of the OMLF, where the intercalants are oriented with some inclination to the host layer in the interlayer space. Details regarding this model and explanation are presented in ref.^[5,6]

Previous studies^[7,8] have shown that the all-trans conformation of the alkyl chains was preferentially adopted and was ordered in two-dimensional lattice when using high-surface charge density clay (such as vermiculite and mica). Osman reported that the average molecular axis of a dioctadecyldimethylammonium cation intercalant is inclined to the mica surface by ca. 50°.^[7] The interdigitated layer structure is of particular importance to understand the intercalation kinetics that can predict final nanocomposite morphology and overall materials properties.

In this paper, in order to prove the importance of the interdigitated layer structure in the direct (melt) intercalation, we report the intercalation of diphenyl sulfide (DFS) molecules into nano galleries based on OMLFs consisting of different types of intercalants and nanofillers with different surface charge density as a reference system of the poly(*p*-phenylenesulfide) (PPS)-based nanocomposite. Although there is no direct correlation between small molecules and macromolecules, the intercalation behavior of the small molecules have a strong impact on the explanation for the intercalation kinetics. We chose an opti-

mal OMLF and conducted the PPS-based nanocomposites preparation with and without shear processing.

Experimental Part

The various types of OMLFs having different types of intercalants used in this study were synthesized by replacing Na⁺ and K⁺ ions in different nanofillers with alkylammonium and alkylphosphonium cations.^[4,9] *n*-Hexadecyltributylphosphonium, octyltriphenylphosphonium (C₁₂TPP), *N*-(cocoalkyl)-*N,N*-[bis(2-hydroxyethyl)]-*N*-methylammonium [qC₁₄(OH)], and octadecylbenzyltrimethylammonium (C₁₈Me₂Bz) cations are miscible with DFS as revealed by melting temperature depression of DFS ($T_m = -21.49$ °C) (Table 1), while octadecylammonium (ODA), octadecyltrimethylammonium (C₁₈TM) cations are immiscible with DFS. Both ODA · Cl⁻ and C₁₈TM · Cl⁻ did not dissolve in DFS. The layer titanate (HTO) is a new nanofiller having high surface charge density^[5] compared with conventional layered silicates [synthetic fluorine hectorite (*syn*-FH) and montmorillonite (MMT)] (Table 2). The mixtures of DFS, purchased from Aldrich, and various OMLFs in weight ratio 70:30 were prepared. The mixtures were stirred for 1 h to obtain homogeneous mixtures and allowed to stand in sealed glass tubes for 3 h at room temperature. The resultant products were isolated by repeated filtration, washed with methanol, and dried at room temperature.^[10] A PPS *fine* powder ($\bar{M}_n = 1.0 \times 10^4$ g · mol⁻¹, $T_m = 285$ °C, purchased from Aldrich), was used. The preparation of the PPS-based nanocomposites was conducted via melt compounding operated at 300 °C for 3 min. The extruded samples were dried under vacuum at 120 °C for 6 h to remove the water. The dried nanocomposites were then converted into sheets with a thickness from 0.7 to 2 mm by pressing with ≈ 1.5 MPa at 300 °C for 1 min using a hot press. To estimate the effect of shear on the nanofiller dispersion, we also conducted nanocomposite preparation without shear processing (just annealed at 300 °C for 30 s). Both types of the sample sheets were then quickly quenched between glass plates and subjected to the characterizations.

Nano structure analyses of WAXD and transmission electron microscopy (TEM) were carried out using the same apparatus as in the previous articles.^[4,9] To investigate the micro-scale morphology of the nanocomposites, we used a polarized optical microscope (POM). The mixture of PPS *fine* powder and OMLFs was first sandwiched between two pieces of cover glass and placed on a laboratory hot plate above the T_m of PPS for 30 s to obtain a thin film of ≈ 30 μm in thickness. The molten film was then rapidly put on a thermostated

Table 1. Melting temperature depression and endothermic heat flow (melting enthalpy) in mixtures of intercalants and DFS (10:90 weight ratio).

	DFS	DFS/C ₁₆ TBPCl ⁻	DFS/C ₁₈ Me ₂ BzCl ⁻	DFS/C ₁₂ TPPCl ⁻
T_m^a / °C	-21.49	-23.12	-22.47	-23.25
ΔH^a / (J · g ⁻¹)	45.06	43.73	37.78	36.46

^{a)} Heating rate is 5 °C · min⁻¹.

Table 2. Characteristic parameters of nanofillers.

Parameters	HTO	syn-FH	MMT
Chemical formula	$\text{H}_{1.07}\text{Ti}_{1.73}\text{O}_{3.95} \cdot 0.5\text{H}_2\text{O}$	$\text{Na}_{0.66}\text{Mg}_{2.6}\text{Si}_4\text{O}_{10}(\text{F})_2$	$\text{Na}_{0.33}(\text{Al}_{1.67}\text{Mg}_{0.33})\text{Si}_4\text{O}_{10}(\text{OH})_2$
Particle size/nm	$\approx 100\text{--}200$	$\approx 100\text{--}200$	$\approx 100\text{--}200$
BET area/($\text{m}^2 \cdot \text{g}^{-1}$)	≈ 2400	~ 800	≈ 700
CEC ^{a)} /[mequiv. \cdot (100 g) ⁻¹]	≈ 200 (660)	≈ 120 (170)	≈ 90 (90)
Surface charge ^{b)} /($e \cdot \text{nm}^{-2}$)	1.26	0.971	0.708
Density/($\text{g} \cdot \text{cm}^{-3}$)	2.40	2.50	2.50

^{a)} Methylene blue adsorption method. Values in parenthesis are calculated from chemical formula of nanofillers.

^{b)} Surface charge density = layer charge/unit cell parameters, a and b .^[5,6,11,13]

hot-stage ($>T_m$) (Linkam RTVMS, Linkam Scientific Instruments, Ltd.) mounted on a POM (Nikon OPTIPHOTO2-POL). Here we briefly describe molecular modeling of the intercalants. Using computer simulation, we proposed the molecular dimensions of two different intercalants, using the molecular dynamics program (MM2 in Quantum Cache, Fujitsu Ltd.) in consideration of van der Waals radii. Optimization of structure is based on the minimization of the total energy of the molecular system.^[6]

Results and Discussion

Intercalation of DFS Molecules into Nanogalleries

WAXD patterns for typical examples of nanofiller powders are presented in Figure 1. The mean interlayer spacing of the (001) plane [$d_{(001)}$] for the HTO modified by C_{16}TBP [HTO- C_{16}TBP], obtained by WAXD measurements is

2.311 nm (diffraction angle, $2\Theta = 3.82^\circ$). The appearance of small peaks observed at $2\Theta = 7.60, 11.36, 15.08,$ and 18.88° have confirmed that these reflections are due to (002) up to (005) plane of HTO- C_{16}TBP . HTO- C_{16}TBP intercalated with DFS [HTO- $\text{C}_{16}\text{TBP}/\text{DFS}$], exhibiting a well-ordered superstructure proved by WAXD with diffraction maxima up to the seventh order due to the high-surface charge density of the HTO layers compared with that of MMT [see Figure 3(a)].

Despite the immiscibility between ODA and DFS, we can see the layer expansion in MMT-ODA after mixing with DFS, indicating the DFS intercalation into nanogalleries. The MMT-ODA/DFS profile shows a less-ordered interlayer structure compared with that of HTO- $\text{C}_{16}\text{TBP}/\text{DFS}$. That is, the coherent order of the silicate layers (MMT) is much lower in each HTO-based OMLFs intercalated with DFS molecules, presumably due to the different surface charge densities.

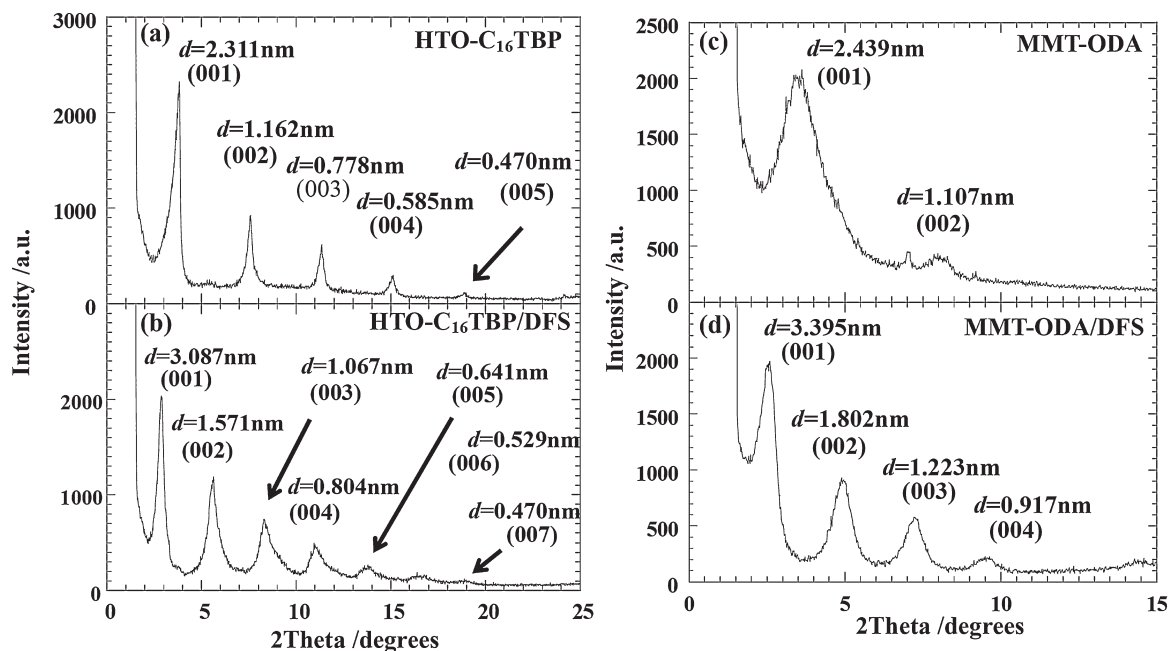


Figure 1. WAXD patterns of (a) HTO- C_{16}TBP , (b) HTO- C_{16}TBP intercalated with DFS, (c) MMT-ODA, and (d) MMT-ODA intercalated with DFS.

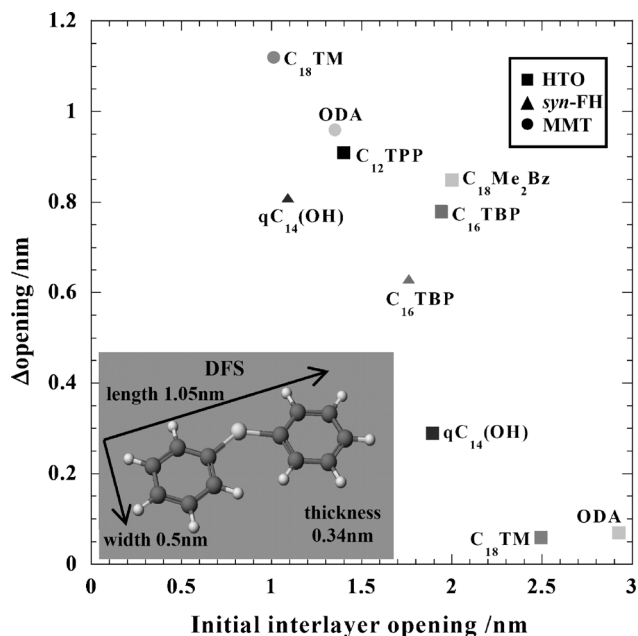


Figure 2. Plot of initial interlayer opening versus Δ opening for various OMLFs intercalated with DFS. The inset shows molecular dimensions of DFS, calculated using a molecular dynamic program (MM2 in Quantum CAChe, Fujitsu Ltd.), taking van der Waals radii into consideration.

In Figure 2, we discuss the change in the interlayer opening, which is estimated after subtraction of the layer thickness value of 0.374 nm for HTO^[11], 0.98 nm for *syn*-FH^[12] and 0.96 nm for MMT.^[13] The intercalation of DFS molecules successfully takes place regardless of the miscibility between DFS and intercalants. Obviously, we

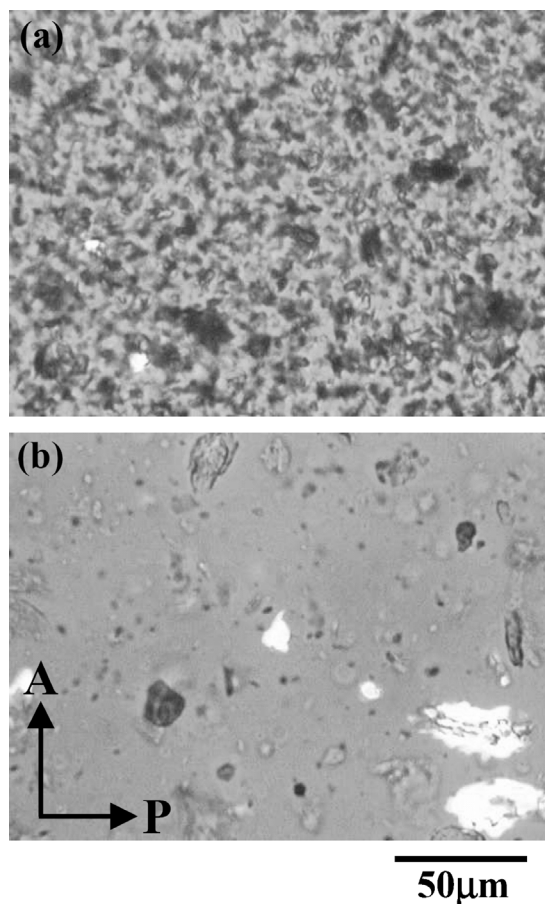


Figure 4. Polarized optical micrographs of (a) PPS/*syn*-FH-C₁₆TBP and (b) PPS/MMT-C₁₆TBP prepared by annealing at 300 °C for 30 s (without shear processing).

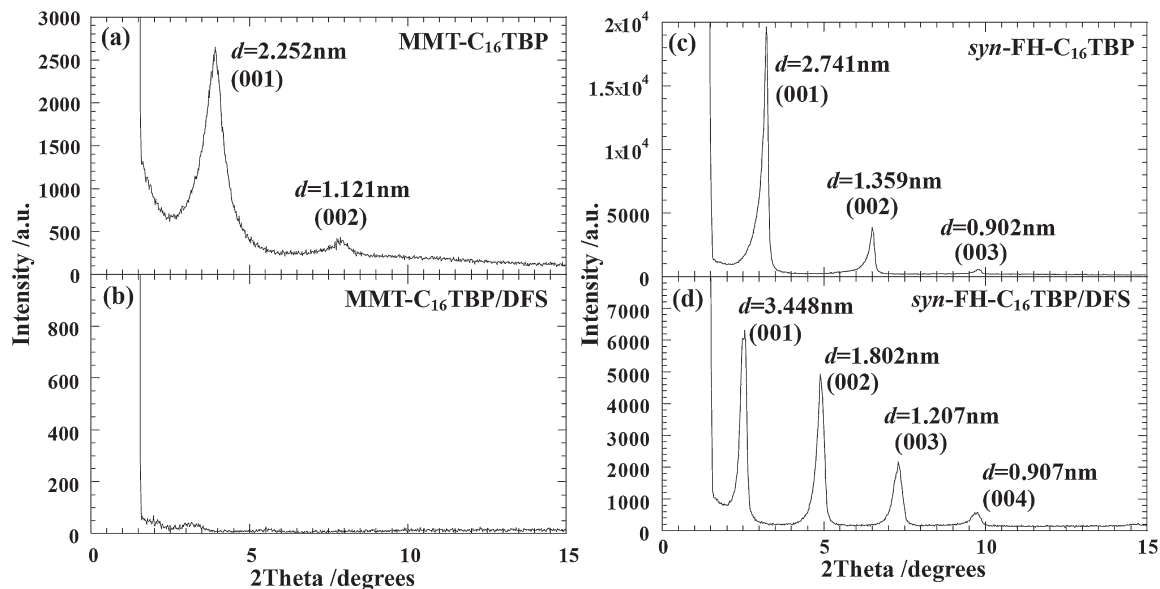


Figure 3. WAXD patterns of (a) MMT-C₁₆TBP, (b) MMT-C₁₆TBP intercalated with DFS, (c) *syn*-FH-C₁₆TBP, and (d) *syn*-FH-C₁₆TBP intercalated with DFS.

can observe the strong correlation between the initial interlayer opening and layer expansion ($=\Delta$ opening) after mixing with DFS. That is, a smaller initial opening leads to a larger interlayer expansion. In other words, the smaller interlayer opening caused by the lower surface charge density and/or short chain length of the intercalant

[e.g., $qC_{14}(OH)$ and $C_{12}TPP$] promotes the large amount of intercalation of DFS molecules, probably due to the configuration with small tilt angle of the intercalant into the nano galleries. This feature has been observed in the results of polyester-based nanocomposites prepared by different OMLFs intercalated with different intercalants.^[5,6]

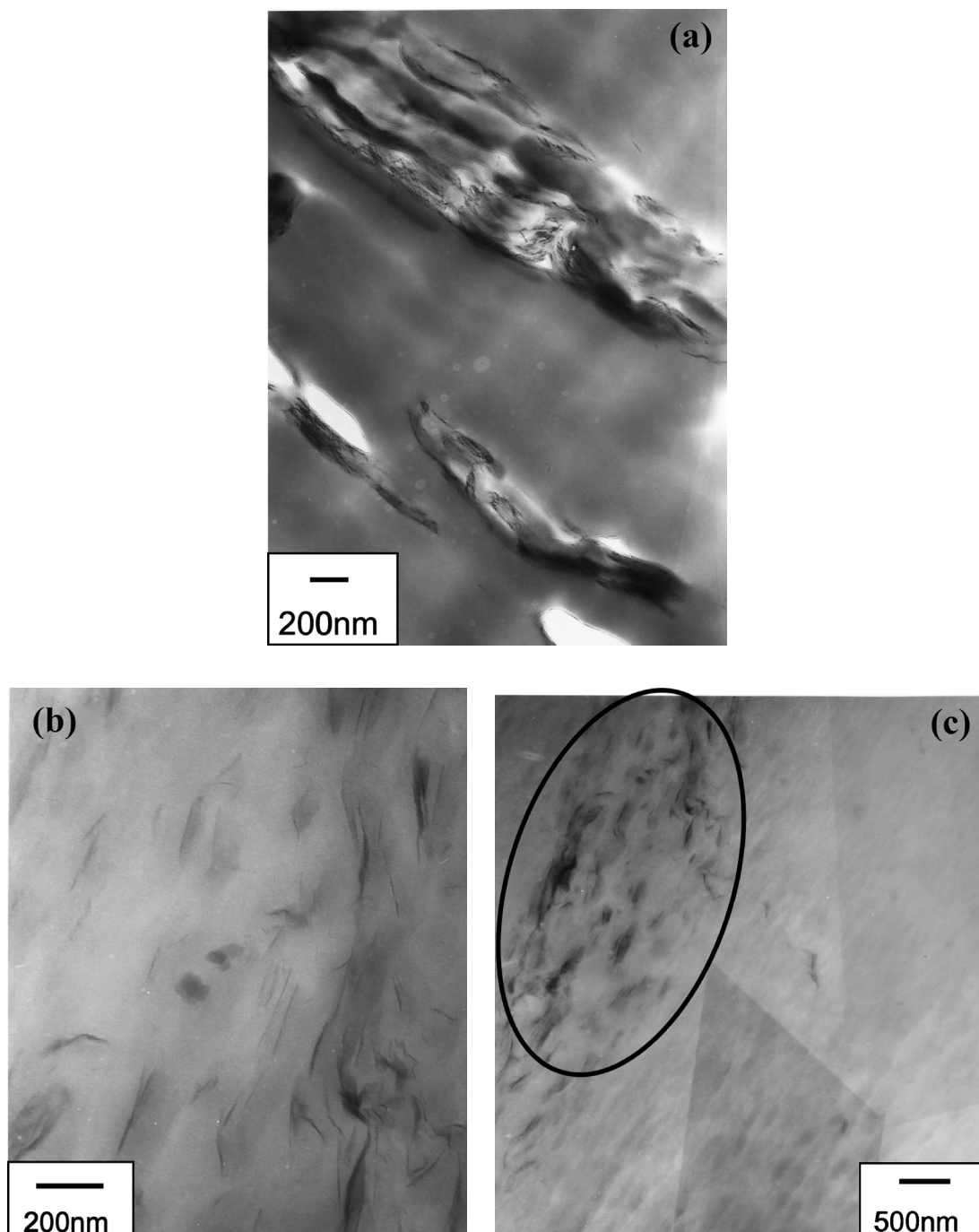


Figure 5. Bright field TEM images of (a) PPS/syn-FH- $C_{16}TBP$, (b) and (c) PPS/MMT- $C_{16}TBP$ prepared by annealing at 300 °C for 30 s (without shear processing). The dark entities are the cross-sections or the faces of intercalated-and-stacked silicate layers, and the bright areas are the matrix. The circled area indicates the aggregated particles containing many discrete silicate layers with finer dispersion (see text).

One more interesting feature is the absolute value of the Δ opening. For HTO-ODA/DFS and HTO- C_{18} TM/DFS, the absolute value of Δ opening [0.07 nm (2.4%) and 0.06 nm (2.4%), respectively] is lower than the molecular dimension of DFS (length, width, and thickness are 1.05, 0.5 and 0.34 nm, respectively) (see the inset in Figure 2). This suggests that the DFS molecules cannot penetrate into galleries when we compare the apparent interlayer expansion ($=\Delta$ opening). It is necessary to understand the meaning of the interlayer expansion in the intercalation. As explained in the first part, we have to take the interdigitated layer structure into consideration. This structure shows the different orientation angles of the intercalants can adopt when DFS molecules penetrate into the galleries. Apparently, the interdigitated layer structure may provide a balance between DFS penetration and different orientation angles of the intercalants.

From these results, the entropic contribution of the intercalants, which leads to the entropy gain associated with the layer expansion after intercalation of the small molecules and/or polymer chains, may not be significant due to the interdigitated layer structure. Presumably, the penetration takes place by the pressure drop into the nano galleries generated by the two platelets.

Effect of Surface Charge Density on Intercalation

For MMT- C_{16} TBP/DFS, the peaks arising from the (001) and (002) reflections of MMT- C_{16} TBP disappear and the

layer structure is destroyed as shown in Figure 3. The delamination and swelling of the MMT layers are retained in the sample. The swelling behavior of the MMT layers was observed by the bare eye. However, the complete exfoliation of the silicate layers is not judged from WAXD analysis. On the other hand, *syn*-FH, which has a higher surface charge density compared with that of MMT, shows intercalated layer structure similar to a HTO- C_{16} TBP/DFS [Figure 3(c) and 3(d)]. This feature has been observed in the result for OMLF modified with $qC_{14}(OH)$. For the same intercalant into the different nanofillers (e.g., comparison among MMT, *syn*-FH and HTO), *syn*-FH- $qC_{14}(OH)$ /DFS exhibits a large value of Δ opening compared with that of HTO- $qC_{14}(OH)$ /DFS. MMT- $qC_{14}(OH)$ /DFS shows the delamination behavior when comparing with *syn*-FH- $qC_{14}(OH)$ /DFS and HTO- $qC_{14}(OH)$ /DFS (data not shown). This indicates that the OMLFs having a lower surface charge density lead to a lower coherent order of the layer structure and the layer structure is presumably destroyed when the OMLFs are modified by some intercalants, which are miscible with the matrix.

PPS-Based Nanocomposite Formation

We conducted nanocomposite preparation without shear processing. Figure 4 shows the morphologies of PPS-based nanocomposites prepared by annealing at 300 °C for 30 s

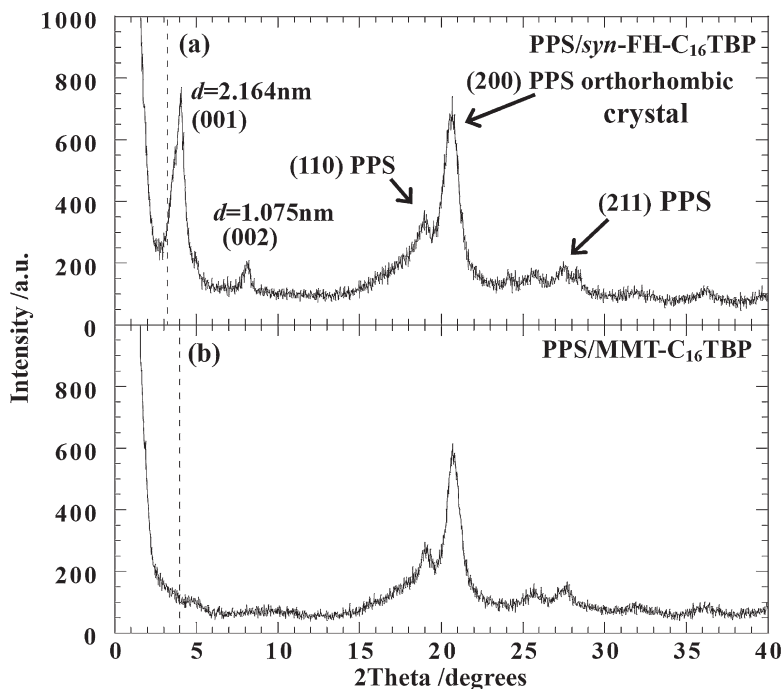


Figure 6. WAXD patterns for PPS-based nanocomposites prepared by (a) *syn*-FH- C_{16} TBP and (b) MMT- C_{16} TBP without shear processing. The dashed line in each figure indicates the location of silicate (001) reflection of each OMLs. The strong diffraction peaks at $2\theta = 15\text{--}30^\circ$ are assigned to the orthorhombic crystal of PPS.

(without shear processing). The OMLS content in the nanocomposites was 5 wt.-%. The alkylphosphonium cation as an intercalant has the advantage of thermal stability compared with the alkylammonium cation.^[6,14] It

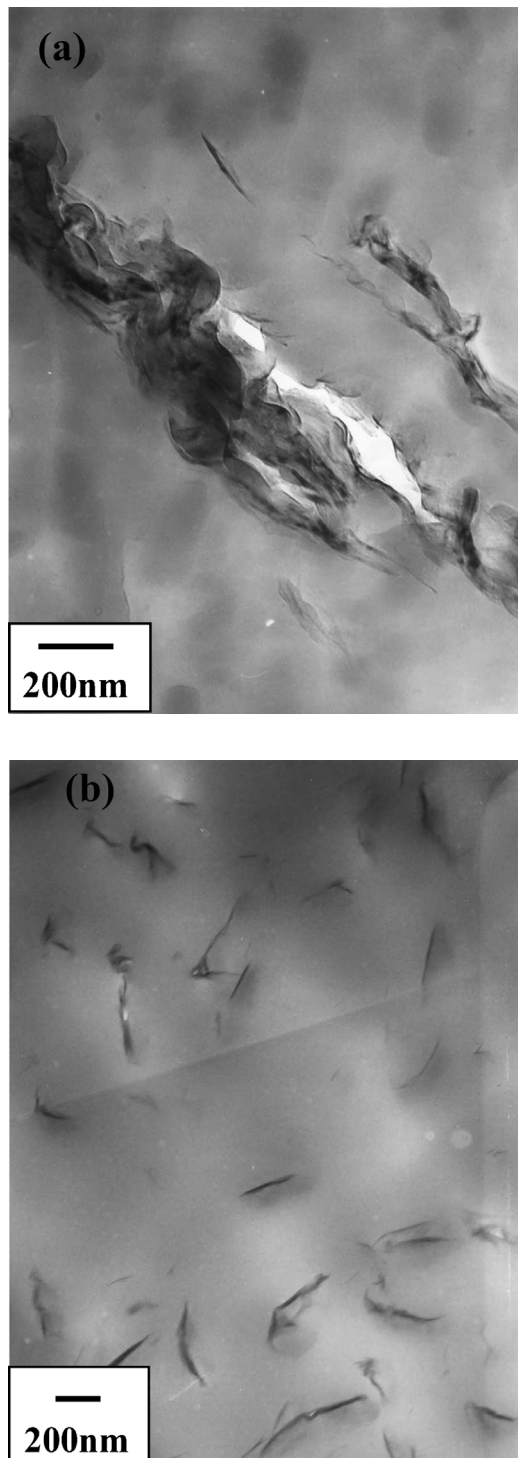


Figure 7. Bright field TEM images of (a) PPS/syn-FH-C₁₆TBP, (b) PPS/MMT-C₁₆TBP prepared by melt compounding with shear (operated at 300 °C for 3 min).

is clear from the POM photographs that stacked-and-agglomerated structure of layers are evident in a PPS/syn-FH-C₁₆TBP system, while good dispersion appears in PPS/MMT-C₁₆TBP systems. The internal structure of the nanocomposites in the nanometer scale was directly observed via TEM analyses.

Figure 5(a) shows the results of TEM bright field images of PPS/syn-FH-C₁₆TBP systems corresponding to the POM experiment, in which dark entities are the cross-sections of the layered nanofillers. The large agglomerated tactoids of about 300 nm thickness are seen in Figure 5(a). On the other hand, Figure 5(b) and 5(c) show the observation of discrete silicate layers. We can observe the aggregated feature of the silicate layers in Figure 5(c). An aggregated particle contains several discrete silicate layers with finer dispersion. For PPS/MMT-C₁₆TBP prepared by annealing without shear processing, the annealing promotes the delamination of the stacked MMT layers. The estimated zero-shear viscosity of the PPS melt ($\bar{M}_n = 1.0 \times 10^4 \text{ g} \cdot \text{mol}^{-1}$) at 300 °C (fitted with Ellis model) was 60 Pa · s.^[15] The intercalation of PPS molecules takes place, presumably due to the low viscosity. This feature greatly resembles the intercalation behavior in OMLS/DFS systems at room temperature. The existence and/or disappearance of sharp Bragg peaks [(001) and (002) planes], in PPS-based nanocomposites prepared without shear processing clearly indicate the dispersed behavior of silicate layers in the PPS matrix (see Figure 6).

Figure 7 shows the results of TEM bright field images of the nanocomposites prepared by melt compounding with shear (operated at 300 °C for 3 min). For PPS/syn-FH-C₁₆TBP, we still observe large stacked silicate layers in the nanocomposites, whereas, in PPS/MMT-C₁₆TBP, a more homogeneously and finely dispersed layer structure is developed when compared with that corresponding to the nanocomposite prepared without shear processing [see Figure 5(b) and 5(c)].

We estimate the form factors obtained from TEM images, i.e., average values of the particle length (L), thickness (D) of the dispersed particles and the correlation length (ξ) between the particles. The details of the evaluation were described in our previous paper.^[9] The results are presented in Table 3. For PPS/MMT-C₁₆TBP prepared by annealing without shear processing, L and D are in the range of (130 ± 50) nm and (9 ± 5) nm, respectively.

Table 3. Form factors of two nanocomposites obtained from TEM observation.

PPS/MMT-C ₁₆ TBP	Without shear ^{a)}	With shear
L/nm	130 ± 50	270 ± 100
D/nm	9 ± 5	22 ± 10
ξ/nm	100 ± 80	350 ± 200

^{a)} The values are obtained from Figure 5(b).

On the other hand, PPS/MMT- C_{16} TBP prepared by shear processing exhibits a large value of L (270 ± 100 nm) with almost double the stacking of the silicate layers ($D = 22 \pm 10$ nm). The ξ value of the nanocomposite without processing (100 ± 80 nm) is lower than the value of the shear processed one (350 ± 200 nm). In case of annealing (without shear), the values are obtained from Figure 5(b). PPS/MMT- C_{16} TBP, after shear processing, exhibiting some staked-and-flocculated silicate layers in the nanocomposite, presumably due to the thermal decomposition of the intercalant (C_{16} TBP) at 300°C . However, a more uniform dispersion of the layers seems to be attained due to the shear processing [cf. Figure 5(c) and 7(b)]. That is, the delamination of the stacked nanofillers is governed by the initial interlayer opening, which is controlled by the surface charge density and molecular dimension of the intercalant, while the uniform dispersion of the nanofillers was affected by the shear processing. The shear stress may have little effect on the delamination of OMLFs in the preparation of PPS-based nanocomposites.

Conclusion

Intercalation of DFS molecules into nano galleries having different initial interlayer opening has been discussed. The small interlayer opening caused by the low surface charge density promoted the large amount of intercalation of DFS molecules regardless of the miscibility between DFS and intercalants. For this reason, PPS-based nanocomposites prepared with MMT- C_{16} TBP without shear processing exhibited finer dispersion. The delamination of the MMT layers was attained when compared with the nanocomposite prepared with *syn*-FH- C_{16} TBP. This approach can be extended to prepare polymeric nanocomposites with finer

dispersion of the nanofillers. This is currently under way in our laboratory and will be clarified shortly.^[16]

Acknowledgements: This work was supported by the MEXT "Collaboration with Local Communities" Project (2005–2009).

- [1] M. Okamoto, "Recent Advances in Polymer/Layer Silicate Nanocomposites: An Overview from Science to Technology", in: *Advances in Processing and Properties of Polymer Nanocomposites*, S. G. Advani, Ed., World Scientific, Singapore 2006.
- [2] R. A. Vaia, E. P. Giannelis, *Macromolecules* **1997**, *30*, 7990.
- [3] R. A. Vaia, E. P. Giannelis, *Macromolecules* **1997**, *30*, 8000.
- [4] R. Hiroi, S. Sinha Ray, M. Okamoto, T. Shiroi, *Macromol. Rapid Commun.* **2004**, *25*, 1359.
- [5] O. Yoshida, M. Okamoto, *Macromol. Rapid Commun.* **2006**, *27*, 751.
- [6] O. Yoshida, M. Okamoto, *J. Polym. Eng.* 2006, in press.
- [7] M. A. Osman, M. Ernst, B. H. Meier, U. W. Suter, *J. Phys. Chem. B* **2002**, *106*, 653.
- [8] M. A. Osman, M. Ploetze, P. Skrabl, *J. Phys. Chem. B* **2002**, *108*, 2580.
- [9] S. Sinha Ray, K. Yamada, M. Okamoto, A. Ogami, K. Ueda, *Chem. Mater.* **2003**, *15*, 1456.
- [10] When these OMLNs are washed with methanol, no change in the WAXD profiles is observed.
- [11] S. Nakano, T. Sasaki, K. Takemura, M. Watanabe, *Chem. Mater.* **1998**, *10*, 2044.
- [12] H. Tateyama, S. Nishimura, K. Tsunematsu, K. Jinnai, Y. Adachi, M. Kimura, *Clays Clay Miner.* **1992**, *40*, 180.
- [13] G. Lagaly, *Clay Miner.* **1970**, *16*, 1.
- [14] P. Maiti, M. Okamoto, K. Yamada, K. Ueda, K. Okamoto, *Chem. Mater.* **2002**, *14*, 4654.
- [15] P. Maiti, M. Okamoto, T. Kotaka, *Polymer* **2001**, *42*, 9827.
- [16] T. Saito, M. Okamoto, in preparation.